Tuning electronic properties of graphene nanoribbons for enhanced detection of toxic gases (F_2, AsH_3, PH_3 and HF): A density functional theory study

R. H. Khalaf and M. L. Jabbar

Department of Physics, College of Science, University of Thi-Qar, Thi-Qar, Iraq.

Received 15 July 2025; accepted 10 October 2025

This study investigates the potential of graphene nanoribbons (GNRs) with zigzag and armchair edge configurations as highly sensitive sensors for toxic gases (F_2, AsH_3, PH_3, and HF) using density functional theory (DFT) with the B3LYP/631G basis set to model and optimize the geometric and electronic structures of pristine and gas-adsorbed GNR compounds. The electronic, structural, and adsorption properties of these GNRs were analyzed to evaluate their gas-sensing performance. Results reveal that zigzag-edged GNRs exhibit superior sensitivity due to their localized edge states, which significantly alter electronic properties upon gas adsorption, particularly for F_2, as evidenced by a notable reduction in the energy gap (from 1.22 eV to 0.97 eV). Meanwhile, armchair paradigms display stable electronic structures with smaller band gap fluctuations (~ 0.5 eV). This means that the armchair-edged GNRs demonstrate greater stability and selectivity, with minimal changes in their electronic structure, suggesting robust sensor performance under ambient conditions. Adsorption energy calculations and infrared spectra further highlight the distinct interactions between the gases and GNRs, with zigzag edges showing stronger responses. Additionally, descriptors such as chemical hardness, softness, electronegativity, and dipole moment provide insights into the reactivity and polarizability of the systems. The findings suggest that zigzag GNRs are promising candidates for high-sensitivity gas sensors, while armchair GNRs may be better suited for robust and selective detection applications. This work contributes to the optimization of graphene-based sensors for environmental and industrial toxic gas monitoring.

Keywords: Graphene; DFT; toxic gases; gas sensing; energy gap.

DOI: https://doi.org/10.31349/RevMexFis.72.021603

1. Introduction

Graphene is a nanomaterial composed of a single atomic layer of carbon atoms arranged in a two-dim nsional hexagonal (honeycomb) lattice. Each carbon atom in the graphene sheet forms three strong covalent σ-bonds with neighboring carbon atoms through sp^2 hybridization, an overlap between one s and two p orbitals while the unhybridized p orbital forms a delocalized π-bond system across the surface [1,2] .This unique electronic configuration contributes to graphene's exceptional stability and conductivity [3]. Due to its remarkable carbon-carbon bond strength $(\sim 4.9\ \mathrm{eV})$ [4], graphene is not only mechanically robust but also exhibits excellent chemical stability. The monolayer of graphene is impermeable to all gases and liquids [5], making it an ideal platform for sensing applications [6]. When a graphene sheet is cut into finite pieces, two distinct edge geometries are formed: zigzag and armchair. These edges play a crucial role in defining the material's electronic and magnetic properties, zigzag edges can host localized [7], nonbonding edge states that exhibit unusual electronic excitations. These excitations can be tuned or manipulated via external electric or magnetic fields or by modifying the sample geometry. In contrast, armchair edges typically lack such edge states, although they do introduce electron wave interference effects during scattering processes [8]. Graphene's unique properties such as ultrahigh electrical conductivity [9], excellent thermal conductivity [10], superior mechanical strength, large surface area-to-volume ratio, and optical transparency make it a highly attractive material for next-generation electronic devices [11]. Among its promising applications, graphene-based sensors for detecting highly toxic gases have attracted growing interest [12]. These gases, often released through industrial processes, pose severe risks to environmental and human health [13]. The core objective of modern sensor development is to achieve ultrasensitive detection [14], ideally down to the level of a single molecule. Graphene's atomic thickness and electronic responsiveness make it a powerful candidate for such highly sensitive detection technologies. Unlike traditional solid-state gas sensors, graphene-based sensors offer improved selectivity, faster response times, and superior signal-to-noise ratios. In light of these characteristics, graphene continues to play a central role in the evolution of nanoscale sensing technologies. Further research is required to optimize its functionalization, improve its selectivity for specific toxic gases, and integrate it into commercial sensor systems [14].

The aim of this study is to simulate and investigate two distinct edge configurations of graphene nano-ribbon (both zigzag and armchair) and evaluate their effectiveness as sensors for selected toxic gases, owing to the critical role these pollutants play in environmental degradation and their harmful effects on living organisms.

2. Computational details

Density functional theory (DFT) is a computational quantum mechanical modeling technique practical to compute the

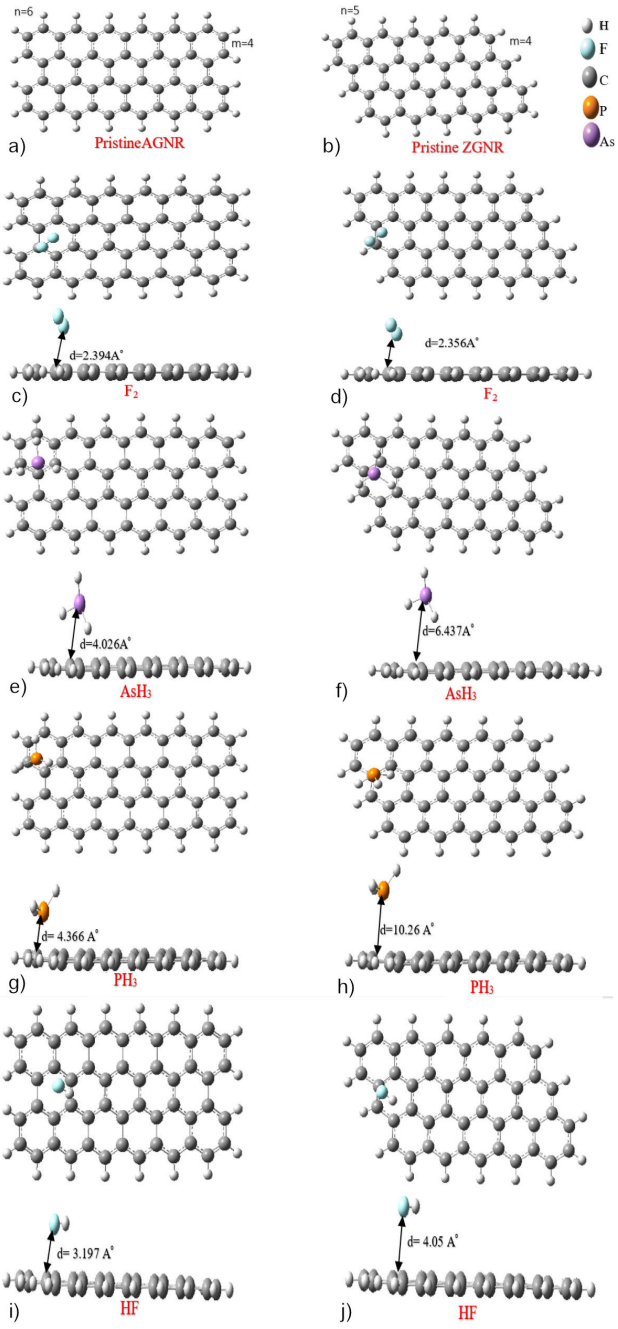

FIGURE 1. Molecular structure for pristine a) AGNR and b) ZGNR adsorption with high toxic gases (a1,b1) F2, (a2,b2) AsH_3, (a3,b3) PH_3 and (a4, b4) HF.

electronic density at each point in space [15–17]. The quantum chemical computation was performed using the $6-31G$. The structure was treated with GNRs , which have zigzag and armchair edges with hydrogen passivation to reduce boundary effects [18], as shown in Fig. 1. The energy of the Fermi level, highest occupied molecular orbital (HOMO) energies, lowest unoccupied molecular orbital (LUMO) energies, and energy gaps represent the electronic properties of GNRs (ZGNR and AGNR) and GNR-X. (Where x symbolizes to toxic gases such as: F_2, AsH_3, PH_3, and HF). To evaluate adsorption parameters such as adsorbent strength between structure GNR and gas atoms energy[19], adsorption distance d was calculated. Adsorption energy is defined by ($E_{ad} = E_{GNR-GAS} - E_{GNR} - E_{gas}$). Three primary areas in which adsorption energy studies are quite helpful are (1) looking into adsorption mechanisms, (2) providing data for chemical engineering, and (3) characterizing the energetic heterogeneity of solid surfaces. The frontier orbital energies are determined under Koopman's approximation. Electronegativity, hardness, softness, and electrophilicity were determined based on the ionization potential (I.P.) and electron affinity (E.A.) values. Essential reactivity indices, including electronegativity χ, chemical hardness η, softness σ, and electrophilicity ω, are described in this theory as derivatives of electronic energy E concerning several electrons N at a constant external potential $v(r)$.

3. Results and discussion

3.1. Molecular structure

DFT was used in computational chemistry programs included in Gaussian 16 with a basis function of $6-31G/B3LYP$ to two types of graphene nanoribbons [16]: the first type, the armchair, which consists of 45 atoms of carbon and 20 atoms of hydrogen ($m = 4$ and $n = 6$); and the second type, the zigzag, which consists of 45 atoms of carbon and 18 atoms of hydrogen ($m = 4$ and $n = 5$). Both compounds consist of carbon atoms in hexagonal rings, and hydrogen atoms are bound to the compound at the outer edges to minimize external influences. The best geometric optimization was achieved until the compound reached its lowest energy, which is the lowest energy, with no imaginary frequencies appearing, as shown in Fig. 1. Both compounds were modeled with toxic gas molecules: F_2, AsH_3, PH_3, and HF, respectively. These gases were chosen because of their high toxicity and double effect (on humans) compared to other toxic gases. Models devoid of imaginary frequencies, which are at the lowest energy, were also adopted. The distance between the gases and the surface of the graphene ribbon was calculated. The gases also showed different distances and angles between the graphene surface and the toxic gas. This is attributed to the interaction between the atoms of the graphene surface and the toxic gas molecules.

3.2. Infrared spectra

Infrared spectra yield harmonic vibrational frequencies. Low frequencies give torsion vibrations. The number of atomic modes depend on the number of atoms in the molecule. Vibration either elastic or inelastic. Obviously, in Fig. 2 the x -axis is frequency ($incm^{-1}$), representing vibrational modes of bonds [20]. While the left of the Y-axis is molar absorptivity ε, showing how strongly the compound absorbs IR at a specific frequency. Also, the right of the Y -axis likely represents IR intensity (D, in $esu^2 \cdot cm^2$), tracking dipole moment

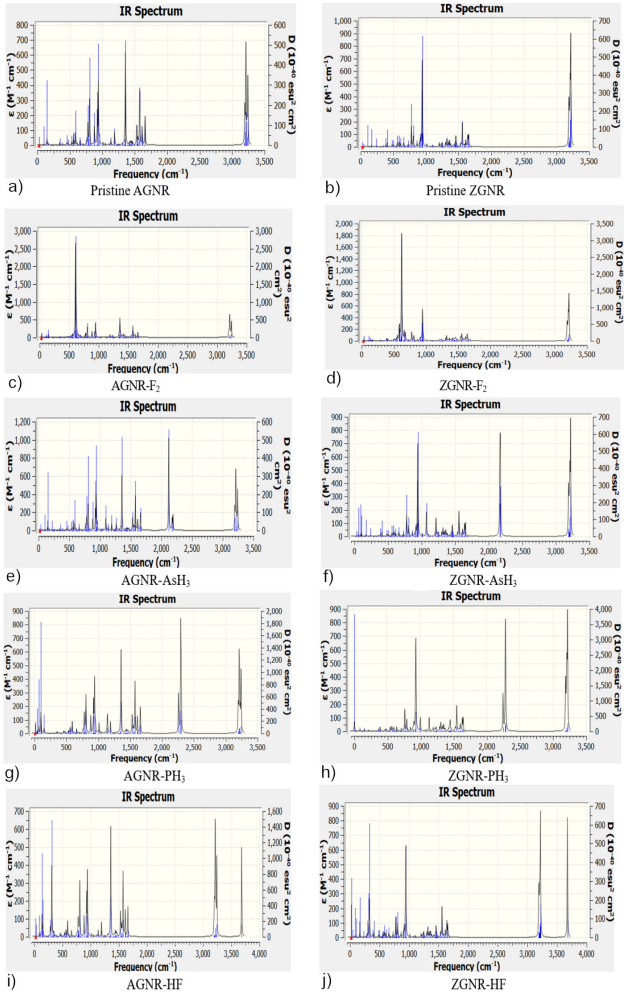

FIGURE 2. Infrared spectra for Pristine a) AGNR and b) ZGNR after adsorption with high toxic gases c), d) F_2, e), f) AsH_3, g), h) PH_3 and i), j) HF.

moment changes during vibration [21]. The first two images represent infrared spectra of two different molecular structures, indicating the graphene compound in both the armchair and zigzag states, without added impurities. A complex aromatic carbon framework (such as the graphene edge) is probably the cause of the wide range of vibrational modes seen in these spectra. Generally, the vibrational modes include bending modes ($\sim 650 - 900\ \mathrm{cm}^{-1}$), potential skeletal vibrations from $\mathrm{C}-\mathrm{H}$ or $\mathrm{C}-\mathrm{C}$, and in-plane $\mathrm{C}=\mathrm{C}$ stretching ($\sim 1,200 - 1,600\mathrm{cm}^{-1}$). Lastly, aromatic ($\mathrm{sp}^2$ carbon) $\mathrm{C}-\mathrm{H}$ stretching modes ($\sim 3,000 - 3,200\ \mathrm{cm}^{-1}$). Both armchair and zigzag graphene nanoribbon configurations respond to adsorption of toxic gases by analyzing their IR spectra. Vibrational modes (especially shifts or new peaks) reveal changes in bonding [22], charge distribution, and molecular interactions. Particularly in the fingerprint range ($400 - 1600\ \mathrm{cm}^{-1}$), zigzag designs exhibit stronger and more distinct peaks. This is probably because zigzag edges have increased electronic activity, which can localize charges and improve infrared sensitivity. Armchair edges, on the other hand, have a somewhat weaker IR reaction because they are often more symmetrical and chemically inert. The toxic gas (like $\mathrm{H}-\mathrm{F}$) stretching vibration is characterized by the sharp peak in both spectra about $3600\ \mathrm{cm}^{-1}$, which verifies that HF is adsorbed on the graphene surface. Variations in position or intensity imply that the strength of interaction differs between armchair and zigzag edges. Modes of HF-graphene interaction, like physisorption or weak hydrogen bonding, may be represented by new peaks in the low-frequency region that are absent from pristine graphene.

3.3. Energy gap

The energy gap is an energy range that separates the conduction band and the valence band. It represents the difference in energy between the two bands, where free electrons cannot exist. This gap determines the type of material whether it is a conductor, insulator, or semiconductor based on its width. Conductors have overlapping conduction and valence bands, resulting in no energy gap Insulators have a gap width of approximately 9 electron volts (eV). Semiconductors have a smaller gap than insulators. The energy gap in graphene is calculated by taking the difference between the energy of the highest occupied molecular orbital (HOMO)and the energy of the lowest unoccupied molecular orbital (LUMO). The energy gap can be expressed mathematically:

The energy gap in material can be mathematically expressed by $E_g = E_{\mathrm{LUMO}} - E_{\mathrm{Homo}}$.

Table I, II indicates that edge geometry (armchair and zigzag) plays a crucial role in modulating the electronic properties of graphene when interacting with toxic gases. While armchair configurations show relatively stable electronic characteristics, zigzag edges exhibit greater responsiveness, especially in band gap variation, suggesting their

TABLE I. Energy of HOMO, LUMO, and energy gap for pristine AGNR and with (F_2, AsH_3, PH_3 and HF), in (electron Volt) unit.

System	E_{Homo}	E_{lumo}	E_{Gap}
P.AGNR	-3.8303	-3.3272	0.5031
AGNR-F2	-4.0067	-3.5136	0.4930
AGNR-AsH 3	-3.8366	-3.3327	0.5039
AGNR-PH3	-3.8238	-3.3213	0.5026
AGNR-HF	-3.9229	-3.4208	0.5020

TABLE II. b. Energy of HOMO, LUMO, and energy gap for pristine ZGNR and with (F2, AsH3, PH3 and HF), in (electron Volt) unit.

System	E_{Homo}	E_{lumo}	E_{Gap}
P. ZGNR	-4.1713	-2.9523	1.2190
ZGNR-F2	-4.3675	-3.3999	0.9676
ZGNR-AsH $_3$	-4.1844	-2.9659	1.2185
ZGNR-PH3	-4.1688	-2.9507	1.2182
ZGNR-HF	-4.3040	-3.0802	1.2239

superior suitability for chemoreceptive or field effect gas sensors. The zigzag graphene shows a significantly larger band gap than the armchair configuration ($\sim$ 1.22 eV vs. $\sim$ 0.50 eV), suggesting stronger localization or edge-state effects. Upon adsorption of F_2, the band gap decreases notably to 0.9676 eV , suggesting a stronger interaction, possibly due to charge transfer or orbital hybridization. HF and As slightly shift the HOMO and LUMO but do not significantly affect the gap, indicating weaker interaction or physisorption. Harvesting: Zigzag edges are more responsive in terms of orbital energy shifts, especially for electronegative species like F_2 and HF.

3.4. Ionization potential and electron affinity, hardness and softness

The higher IP means the structure is less likely to lose electrons. In the context of sensors, a lower IP can enhance charge transfer to the substrate, increasing sensitivity, while the ability of system to accept electrons. Higher EA values are indicative of better electron capturing behavior, essential for detecting electron donating gases, while the system's capacity to take in electrons. Better electron-capturing activity, which is necessary for identifying gases that donate electrons, is indicated by higher EA values. The reactive, while a soft molecule is more polarizable and chemically active. The softness ($\sigma = 1/\eta$) is given by the inverse of hardness. Soft systems are more responsive to external perturbations critical in sensor applications.

Table III, shows the chemical hardness η for armchair systems occurs within a narrow band ($\sim 0.246 - 0.252$eV), regardless of the gas. This indicates structural and electronic robustness of the armchair edge under perturbation. Softness σ remains close to 2.0eV^{-1}, indicating these structures are inherently soft but less variable upon gas adsorption. Thus, zigzag edges are known for their localized electronic edge states. These states contribute to higher baseline hardness (~ 0.61eV) in the undoped system implying less polarizability and more inert character initially. Upon F_2 adsorption, η drops significantly from 0.6095 to 0.4838 eV , and σ increases to 1.0335 eV^{-1}. This means that F_2 substantially activates the zigzag edge, promoting charge redistribution. Similarly, EA increases to 3.3999 eV, showing enhanced electron-accepting character Table IV. Harvesting, F_2 triggers the largest shift in both types due to its high electronegativity, confirming that F- containing species (*e.g.*, HF) are ideal targets for graphene-based gas sensors. While, other toxic gases such as AsH_3 and PH_3 produce minimal electronic changes, suggesting low affinity or weak interaction, and therefore may require functionalization to improve sensitivity.

3.5. Electronegativity χ, electrophilicity ω, polarizability α and dipole moment μ

Significant changes in the electronic characteristics of AGNR and ZGNR following the adsorption of F_2, AsH_3, PH_3, and HF are shown by the findings in Table V. When compared to the pristine ribbons, the electronegativity χ generally exhibits a modest increase. The most noticeable boost is shown for HF adsorption, namely in ZGNR-HF. This suggests that the adsorbed systems have a greater propensity to draw electrons. Likewise, upon adsorption, the electrophilicity index ω rises, indicating enhanced electron-accepting capacity, with ZGNR-HF once more displaying the greatest value. In contrast, the polarisability α values stay within a small range $\approx 770 - 885$ a.u., suggesting that adsorption has a little impact on the sensitivity to external electric fields and total electronic delocalisation. The dipole moment μ exhibits the most notable variation.

TABLE III. Ionization potential in (eV), Electron Affinity in (eV), Hardness η in (eV) and Softness σ in (eV^{-1}) for pristine AGNR and with (F_2, AsH_3, PH_3 and HF).

System	I.P.	E.A.	η	σ
P.AGNR	3.8304	3.3272	0.2516	1.9876
AGNR-F2	4.0067	3.5136	0.2465	2.0282
AGNR-AsH3	3.8366	3.3327	0.2520	1.9844
AGNR-PH3	3.8238	3.3213	0.2513	1.9898
AGNR-HF	3.9229	3.4208	0.2510	1.9919

TABLE IV. b. Ionization potential (IP) in (eV), electron affinity (EA) in (eV), Hardness $\eta(\text{eV})$ and Softness σ (eV^{-1}) for ZGNR and ZGNR with (F_2, AsH_3, PH_3 and HF).

System	I.P.	E.A.	η	σ
P.ZGNR	4.1713	2.9523	0.6095	0.8203
ZGNR-F2	4.3675	3.3999	0.4838	1.0335
ZGNR-AsH 3	4.1844	2.9659	0.6092	0.8207
ZGNR-PH3	4.1688	2.9507	0.6091	0.8209
ZGNR-HF	4.3041	3.0802	0.6120	0.8170

TABLE V. Electronegativity χ, electrophilicity (ω), polarizability α and Dipole moment μ for pristine AGNR and ZGNR with (F_2, AsH_3, PH_3 and HF).

System	$\chi(\text{eV})$	$\omega(\text{eV})$	α (a.u)	$\boldsymbol{\mu(\mathbf{D})}$
P. AGNR	-3.579	25.457	836.7	0.0
AGNR-F2	-3.760	28.676	885.9	4.790
AGNR-AsH3	-3.585	25.499	854.5	0.345
AGNR-PH3	-3.573	25.396	860.9	1.159
AGNR-HF	-3.672	26.856	839.6	2.445
P. ZGNR	-3.562	10.407	775.7	0.0
ZGNR-F2	-3.884	15.588	796.8	4.011
ZGNR-AsH3	-3.575	10.490	795.0	0.693
ZGNR-PH3	-3.560	10.402	794.6	1.237
ZGNR-HF	-3.692	11.138	778.3	2.914

Pure AGNR and ZGNR have very little dipole moments, however adsorption adds a lot of polarity. Strong charge redistribution within the systems is reflected in the greatest dipole moments (4.79 Debye for AGNR-HF and 2.91 Debye for ZGNR-HF) caused by HF adsorption. Overall, the findings show that while polarisability is essentially unaltered, adsorption, particularly with HF, significantly increases the electronegativity, electrophilicity, and dipole moment of nanoribbons.

3.6. Density of states DOS

In quantum mechanics, the waves of a system (particles) can occupy specific states and configurations permitted by the system, with quantized wavelengths determined by the system [23]. The direction of wave propagation is constrained in certain systems. Thus, some systems only allow wave propagation in a single direction, which is attributed to the crystalline structure of the materials. The DOS for a system is a critical property in material physics [24]. When an energy level is permitted for electron occupation in the system, the density of states refers to the number of available states per energy unit at each level.

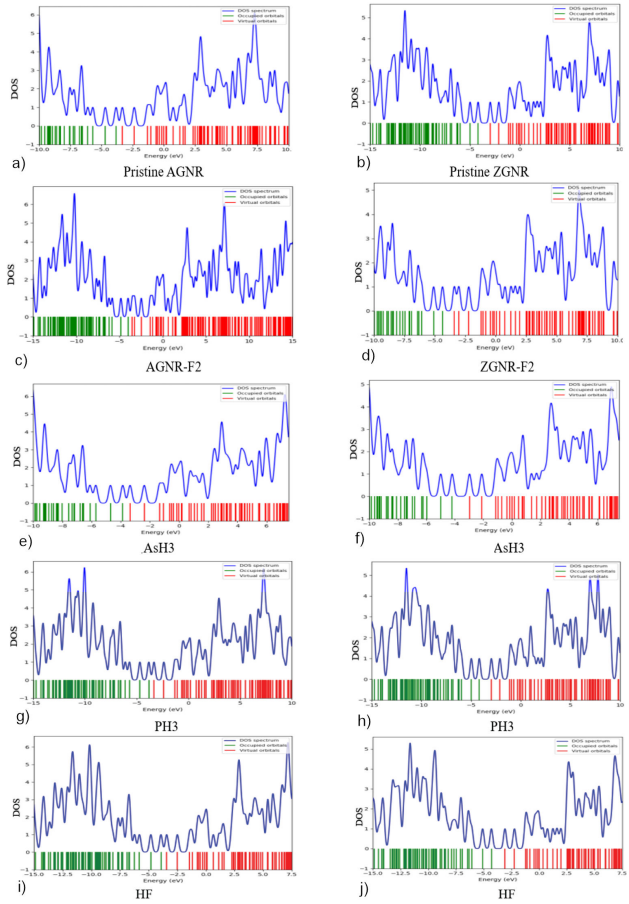

FIGURE 3. Density of states for a) AGNR and b) ZGNR after adsorption with high toxic gases c), d) F2, e), f) AsH_3, g), h) PH_3, and i), j) HF.

In Fig. 3, it can be seen that the vertical axis represents the density of states (DOS), *i.e.*, the number of orbitals available for each energy level. The horizontal axis indicates the energy levels, measured in eV . The green lines represent occupied orbitals, while the red lines represent unoccupied orbitals. The blue line represents the final electron probability, which is used to understand the electronic behavior of a material by displaying the number of available electronic states at each energy. The armchair compound has a noticeable energy gap, a consistent electron distribution, and serves as a perfect model for semiconductors, making it great for detecting gases, especially AsH_3 or pH_3. however, are strongly edgedependent and exhibit greater DOS disturbances, making them more reactive but relatively less stable.

3.7. Adsorption energy (E_{ads}) and percentage of energy gap change

The adsorption energy (Eads) and the energy difference (ΔE) associated with the interaction of functionalized graphene structures specifically Armchair and Zigzag edge configurations with various toxic gas [25] molecules such as, F_2, AsH_3, PH_3 and HF. Where adsorption energy is a critical parameter in assessing the strength of interaction between a gas molecule and a material surface. A more negative value of Eads represents stronger binding and often suggests a chemisorption process, whereas less negative values represent physisorption [26].

$$\Delta \mathrm{E} = \mathrm{E}_{\mathrm{GNR}} - \mathrm{E}_{\mathrm{GNR\text{-}gas}} * 100\% \ldots .2.$$

In general, Armchair graphene consistently shows slightly higher (more negative) adsorption energies, suggesting stronger binding due to favorable local orbital overlap at the edge structure. While Zigzag graphene displays nearly equivalent performance, enhanced the conclusion that both edge types are viable platforms for adsorptionbased sensing applications. Table VI presents both Armchair and Zigzag graphene, the weakest interaction is observed with HF molecules, with Eads values around -0.13 eV, indicat-

TABLE VI. Adsorption energy and percentage of energy gap change for pristine AGNR and ZGNR with (F2, AsH_3, PH_3 and HF).

System	$\mathrm{E}_{\mathrm{ads}}$ (eV)	ΔE(eV)
P.AGNR	.....	....
AGNR-F2	-0.3094	10.015
AGNR-AsH3	-1.9281	112.14
AGNR-PH3	-1.3025	17.213
AGNR-HF	-0.1315	5.0372
P.ZGNR	....	....
ZGNR- F2	-0.3011	11.312
ZGNR-AsH3	-1.8420	126.75
ZGNR-PH3	-1.2661	19.455
ZGNR-HF	-0.1395	5.6936

ing weak physisorption. Adsorption becomes significantly stronger with PH_3 (Eads ≈ -1.3 eV) and is most pronounced with AsH_3 (Eads ≈ -1.9 eV), demonstrating chemisorption behavior likely due to the lone-pair interactions and the larger atomic radii of as atoms, which facilitate overlap with graphene π-orbitals. The ΔE values reflect the total energy change in the system as a result of gas adsorption. This includes structural relaxation and electronic redistribution, serving as an indicator of system stability post-adsorption. For instance, the molecules of AsH_3-functionalized systems exhibit the highest $\Delta E(\sim 112.14, 126.75$ eV), suggesting significant stabilization and strong molecule (toxic gas) surface interactions. This makes these systems excellent candidates for sensing As-containing compounds. The structures interacting with PH_3 also exhibit a substantial energy change ($\sim$ 17.213, 19.455 eV), reinforcing their potential as sensitive sensors. Comparatively, HF causes only modest changes in energy (~ 5 eV), indicating minimal disturbance to the structure, which may result in lower sensor responsiveness. Harvesting Pristine AGNRs and ZGNRs are stable with low dipole moments and distinct band gaps (~ 0.5 eV and ~ 1.22 eV, respectively). Gas adsorption leaves AGNRs mostly unchanged, showing robustness and selectivity, while ZGNRs undergo stronger electronic and vibrational perturbations, especially with F_2, which notably reduces the band gap. Adsorption energies reveal weak HF binding but strong chemisorption with AsH_3 and PH_3. Thus, AGNRs are stable and selective, whereas ZGNRs are more reactive and highly sensitive, making them superior for toxic gas sensing.

4. Conclusions

Zigzag configurations are better suited for highsensitivity sensing applications, while armchair systems may be preferable for robust and selective detection in integrated sensor platforms. In contrast to AGNRs, ZGNRs exhibit substantial sensitivity to F_2, as evidenced by distinct changes in both η and σ. The little alterations for AsH_3, PH_3, and HF indicate the possibility of selective detection, especially for halogenated toxic gases. The high adsorption energies and ΔE values underscore the potential of these structures for toxic gas sensing applications, particularly for the detection of toxic gases such as AsH_3. Furthermore, the similarity in performance between armchair and zigzag edges provides flexibility in structural design, allowing optimization based on fabrication constraints without sacrificing sensitivity.

Acknowledgment

This research is supported by the Department of Physics, College of Science, University of Thi-Qar, Thi-Qar, Iraq as part of Master research graduation requirements.

Author contribution

L. J.: Supervised the research project, analysis the results, and wrote the article; **R. H. K.:** performed the calculations and wrote the manuscript, data interpretation and discussion of the results.

Funding

No funding was received.

Conflict of interest

The authors declare there is no conflict of interest.

Data availability

The data supporting the findings of this study are available within the article upon request.

1. Y. Kumar, S. Sahoo, and A. K. Chakraborty, Mechanical properties of graphene, defective graphene, multilayer graphene and SiC -graphene composites: A molecular dynamics study, *Physica B: Condensed Matter*, **620** (2021) 413250, https://doi.org/10.1016/j.physb.2021.413250

2. M. Gyan, A Study on Two Dimensional (2D) Piezoelectric Semiconductor Materials: A Review, *University of Thi-Qar Journal of Science*, **12** (2025) 102-113, https://doi.org/10.32792/utq/utjsci/v12i1.1329

3. Z. Zhen and H. Zhu, Structure and properties of graphene, in Graphene: (Elsevier, 2018) 1-12. https://doi.org/10.1016/B978-0-12-812651-6.00001-X

4. G. A. Rance, D. H. Marsh, R. J. Nicholas, and A. N. Khlobystov, UV-vis absorption spectroscopy of carbon nanotubes: Relationship between the π electron plasmon and nanotube diameter, *Chemical Physics Letters*, **493** (2010) 19-23, https://doi.org/10.1016/j.cplett.2010.05.012

5. Y. Liu, B. Xie, Z. Zhang, Q. Zheng, and Z. Xu, Mechanical properties of graphene papers, *Journal of the Mechanics and Physics of Solids*, **60** (2012) 591-605, https://doi.org/10.1016/j.jmps.2012.01.002

6. N. Melnikova, V. Egorushkin, N. Bobenko, and A. Ponomarev, The density of states and thermopower in disordered carbon nanotubes, *Russian Physics Journal*, **55** (2013) 1266-1277, https://doi.org/10.1007/s11182-013-9955-1

7. T. Enoki, S. Fujii, and K. Takai, Zigzag and armchair edges in graphene, *Carbon*, **50** (2012) 3141-3145, https://doi.org/10.1016/j.carbon.2011.10.004

8. J. Kim *et al.*, Distinguishing zigzag and armchair edges on graphene nanoribbons by X-ray photoelectron and Raman spec-

troscopies, *ACS omega*, **3** (2018) 17789-17796, https://doi.org/10.1021/acsomega.8b02744

9. H. Hameed and H. A. Yasser, Three-Layers Slab Waveguide with Chiral Metamaterial Core and Graphene Interfaces, *University of Thi-Qar Journal of Science*, **11** (2024) 97-102, https://doi.org/10.32792/utq/utjsci/v11i2.1254
10. A. Nag, A. Mitra, and S. C. Mukhopadhyay, Graphene and its sensor-based applications: A review, *Sensors and Actuators A: physical*, **270** (2018) 177-194, https://doi.org/10.1016/j.sna.2017.12.028
11. D. Sergeyev, L. Myasnikova, and K. S. Shunkeyev, Computer simulation of spin filtration properties of zigzag-edged octagraphene nanoribbon saturated with hydrogen atoms, *Russian Physics Journal*, **63** (2020) 303-310, https://doi.org/10.1007/s11182-020-02036-0
12. K. Toda, R. Furue, and S. Hayami, Recent progress in applications of graphene oxide for gas sensing: A review, *Analytica chimica acta*, **878** (2015) 43-53, https://doi.org/10.1016/j.aca.2015.02.002
13. S. R. Shin *et al*., Graphene-based materials for tissue engineering, *Advanced drug delivery reviews*, **105** (2016) 255-274, https://doi.org/10.1016/j.addr.2016.03.007
14. N. Hu *et al*., Gas sensor based on pphenylenediamine reduced graphene oxide, *Sensors and Actuators B: Chemical*, **163** (2012) 107114, https://doi.org/10.1016/j.snb.2012.01.016
15. N. Ali, L. F. Al-Badry, and A. B. Ahmed, DFT Study in Strain Engineering HfSe2 Nanosheets for Sensing SO2, SOF2, and SO2F2 Gases, *University of Thi-Qar Journal of Science*, **12** (2025) 224-232, https://doi.org/10.32792/utq/utjsci/v12i1.1393
16. A. Ali and N. A. Toama, DFT study of Mn-doped CeO2: The structural and electronic properties, *University of Thi-Qar Journal of Science*, **11** (2024) 190-196, https://doi.org/10.32792/utq/utjsci/v11i2.1252
17. M. L. Jabbar and K. J. Kadhim, Electronic properties of doped graphene nanoribbon and the electron distribution contours: A DFT study, *Russian Journal of Physical Chemistry B*, **15** (2021) 46-52, https://doi.org/10.1134/S1990793121010188
18. H. Fadel and M. Abd-AlHussien, Theoretical Study of External Electric Field Effect on the Chemisorption of a Spherical Semiconducting Quantum-dot on Graphene, *University of Thi-Qar Journal of Science*, **11** (2024) 36-44, https://doi.org/10.32792/utq/utjsci/v11i1.1164
19. W. Tian, X. Liu, and W. Yu, Research progress of gas sensor based on graphene and its derivatives: A review, *Applied Sciences*, **8** (2018) 1118, https://doi.org/10.3390/app8071118
20. Q. Guo, C. Li, B. Deng, S. Yuan, F. Guinea, and F. Xia, Infrared nanophotonics based on graphene plasmonics, *ACS Photonics*, **4** (2017) 2989-2999, https://doi.org/10.1021/acsphotonics.7b00547
21. S. Kyrkjebø *et al*., Graphene and graphene oxide on Ir (111) are transparent to wetting but not to icing, *Carbon*, **174** (2021) 396-403, https://doi.org/10.1016/j.carbon.2020.12.030
22. Y. Ohno, K. Maehashi, and K. Matsumoto, Chemical and biological sensing applications based on graphene field-effect transistors, *Biosensors and Bioelectronics*, **26** (2010) 1727-1730, https://doi.org/10.1016/j.bios.2010.08.001
23. S. Sahu and G. Rout, Band gap opening in graphene: a short theoretical study, *International Nano Letters*, **7** (2017) 81-89, https://doi.org/10.1007/s40089-017-0203-5
24. K. Nakada and A. Ishii, DFT calculation for adatom adsorption on graphene, in Graphene Simulation: (IntechOpen, 2011). https://doi.org/10.5772/20477
25. C. Thierfelder, M. Witte, S. Blankenburg, E. Rauls, and W. Schmidt, Methane adsorption on graphene from first principles including dispersion interaction, *Surface Science*, **605** (2011) 746-749, https://doi.org/10.1016/j.susc.2011.01.012
26. K. Nakada and A. Ishii, Migration of adatom adsorption on graphene using DFT calculation, *Solid State Communications*, **151** (2011) 13-16, https://doi.org/10.1016/j.susc.2011.01.012